Experimental Study of the Critical Speed Response, of a Jeffcott Rotor with Acceleration

by H. L. HASSENPFLUG, R. D. FLACK *and* E. J. GUNTER

Department of Mechanical and Aerospace Engineering, School of Engineering and Applied Science, University of Virginia, Charlottesville, VA 22901, U.S.A.

ABSTRACT: *A small, lightly damped rotor ($\zeta = 0.0088$) was experimentally tested for a variety of acceleration and deceleration rates. In each case, the amplitude response was plotted as a function of operating speed, with the acceleration rate considered. In each case the results are compared with theoretical predictions. The results agree within 6% at the peak response. The results of the analysis indicate that for high acceleration rates the critical amplitude response may be reduced by a factor of four or more. The frequency of the effective critical speed may be shifted by up to 20%. Furthermore, a beating frequency was observed in the amplitude data after the rotor had passed through the critical speed. This phenomenon is shown to be the vector sum of a synchronous component of amplitude and a nonsynchronous transient component (at the critical speed). The transient non-synchronous component is shown explicitly via electronic band-pass filtering, as is the forced response component. Finally, spectral analyses were performed over a range of operating speeds, yielding waterfall diagrams and further verification of the existence of the two components.*

Nomenclature

A	Amplification factor, δ/e
A_{cr}	Amplification factor at ω_{cr} with no acceleration
A_{max}	Maximum amplification factor during acceleration
e	Unbalance eccentricity
f	Frequency
α	Angular acceleration
δ	Deflection at center of shaft
ζ	Normalized damping, $1/(2A_{cr})$
ω	Operating rotational speed
ω_{cr}	Umdamped system critical speed
ω_{max}	Operating rotational speed at A_{max}.

I. Introduction

Most high speed power generating equipment includes rotors which operate above one or more resonances. Previously, several authors have found that if a rotor is accelerated rapidly through a critical speed, the machine's maximum response to unbalance can be controlled. Thus, the machine can be operated

safely on run-up and at the operating speed. However, the deceleration rates on many machines are not controllable. Since deceleration rates are generally slower than acceleration rates, resonant problems may be encountered on run-down, where they may have been avoided on run-up, causing machine damage.

The phenomenon of acceleration through resonance was investigated analytically via a convolution integral by Lewis (**1**). His solution displays the amplitude of vibration as a function of non-dimensionalized operating speed. He employed a forcing function of constant amplitude, i.e. it did not vary with speed as in a real unbalance force. When mass unbalance is considered as a forcing function, the amplitude varies as the square of the operating speed. As a result, his results may lead to significant errors when applied to a rotor system. Furthermore, Lewis deals only with the amplitude of response and does not address the phase relationship between unbalance and rotor response.

Baker (**2**) studied the acceleration of a rotor using mechanical analog to solve the model equations. However, the range of acceleration rates which he employed was out of range for most machinery. Also, he did not include any predictions for very lightly (but non-zero) damped cases. Unfortunately, these are the machines on which acceleration has the most pronounced effect. Phase relations were also not considered in (**2**).

Meuser and Weibel (**3**) studied accelerating systems with non-linear spring rates via a mechanical analog. A constant forcing function was used similar to that in (**1**). Primarily, this reference deals with the effects of non-linearities rather than acceleration rates.

Gasch *et al.* (**4**) consider acceleration of a rotor under the assumption of constant torque, allowing the acceleration to vary as torque is absorbed in resonant response. Their work avoids the range of practical application by assuming large unbalance eccentricities and very large acceleration rates. Both of these assumptions fall outside of the realm of most machine applications. The authors also only present results for the amplitude of the response; phase is not considered, nor is the speed at which maximum response occurs.

Hassenpflug *et al.* (**5**), presented both theoretical and experimental results for a Jeffcott rotor. They used a finite difference technique to solve the equations of motion and presented both amplitude and phase response predictions. The technique was applied to a simple single mass rotor on rigid supports, and is much more versatile than the methods used in (**1–4**). For example, the same technique could be applied to a multimass system on fluid film bearings. These authors (**5**) indicated that two components of response were present: one at the operating speed (unbalance response) and one at the critical speed. In (**5**) only minimal experimental data was presented. The data that was presented indicated good agreement with the theoretical predictions, but a complete experimental analysis of the data was not included.

The objective of this paper is to provide a detailed experimental analysis of results measured in an actual rotor system. Results are compared with theory over a wide range of acceleration rates. Also, the data is analyzed spectrally to show the transient and forced response components of motion.

II. Experimental Apparatus and Analysis

The test rig

The experimental rotor employs a single unbalanced disk, centrally mounted on a flexible shaft which is in turn symmetrically mounted on rigid porous bronze bearings (see Fig. 1). The system parameters are as follows: Length: 40.6 cm; disk mass: 1.41 kg; shaft diameter: 9.53 mm; and critical speed: 1730 rpm.

The rig was instrumented with three displacement transducers. Two were located near the mass and the third was placed over a notch on one end of the shaft. The two central probes were calibrated and particular probes were chosen such that the two calibration curves were matched. Thus, direct comparison of the outputs of the X and Y probes was possible.

Data was analyzed using a synchronous tracking filter (see Fig. 1). The notch on the shaft was used as the trigger for the tracking filter. Outputs from the tracking filter included total or synchronous amplitude and synchronous phase angle (measured with respect to the notch). Reduced data was plotted using an analog plotter. Raw signals from the displacement probes were recorded on a FM tape recorder so that permanent records were obtained.

The rig was first run for negligible acceleration. A mass unbalance vector of 0.010 mm was used and the bow vector was less than 0.003 mm. From this base run, the system damping was determined. First, the response at the critical speed was divided by the response at four times the first critical speed. The latter corresponds to the mass unbalance vector. This generated a nondimensionalized critical speed response of 59.0, which corresponds to a damping

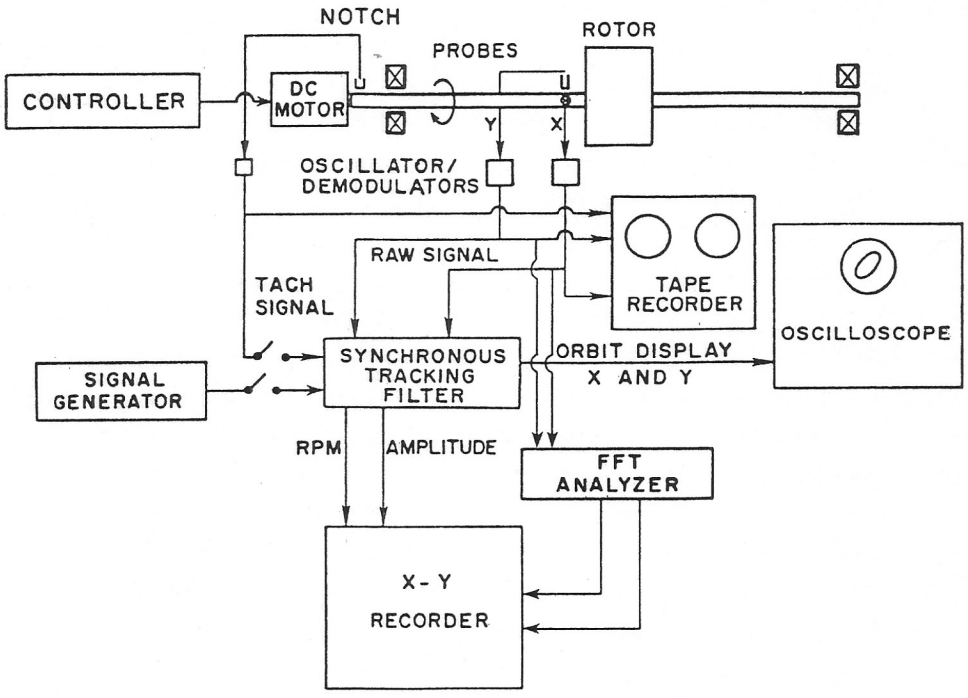

FIG. 1. Test rotor and instrumentation.

ratio of 0.0085. Secondly, the slope of the phase angle versus speed curve was used to calculate ζ by:

$$\zeta = (\mathrm{d}\phi/\mathrm{d}\omega)_{cr}^{-1} \times \omega_{cr}^{-1}. \tag{1}$$

From (1), the value of ζ was found to be 0.0091. Thus, since a difference of less than 7% was found, an average of the two methods was used to define the damping: $\zeta = 0.0088$, $A_{cr} = 57$. The bow and unbalance vectors were held constant for the remainder of the tests.

Procedure

Several tests were performed including acceleration and deceleration runs. The procedure of each run was as follows:

(i) A steady state operating speed was attained well out of the range of the critical speed, such that start up transients would not affect the critical speed response. For acceleration runs this speed was 0.5 ω_{cr} while for the deceleration runs the speed was 1.5 ω_{cr}.

(ii) The rotor system was run through the critical speed at some acceleration rate varied by the controller. The controller operated by placing a variable resistor in parallel with the motor windings. Raw data was recorded with the FM tape recorder.

Analysis

Upon playback the data was analyzed by several methods. First, it was fed into a synchronous tracking filter. The synchronous tracking filter could be used in two modes: narrow band pass around the operating speed or an infinitely wide band pass, i.e. no filtering. In the first mode a signal proportional to the synchronous amplitude is output, while in the second mode a signal proportional to the total amplitude is output. The total signal (synchronous + nonsynchronous components) was plotted first and compared to the theoretical results of (**5**) for the various acceleration rates. The acceleration rates were determined by graphical differentiation of rotational speed versus time plots.

Second, a narrow band-pass synchronous tracking filter (0.8 Hz bandwidth) which operated at the machine running speed was used with the signal. This had the effect of eliminating all non-synchronous components of motion from the output.

Third, a narrow band-pass filter was again used and the same input signals were run again. This time the band pass filter was tuned to the system critical speed rather than operating speed (Fig. 1). For this method of analysis, a waveform generator was employed. From this analysis only the transient component of motion at the critical speed was seen. Finally for comparison, the results of each of the three analyses were plotted on the same non-dimensionalized graph.

As a fourth mode of analysis, the recorded data was fed into a Fast Fourier Transform (FFT) analyzer for a variety of operating speeds taken over each

respective run. The results were then displaced vertically in accordance with operating speed to provide waterfall diagrams.

Lastly, the complete waveforms (raw data) were plotted in the vicinity of the critical speed to show the changing frequency and fluctuations in amplitude which resulted. This last method of analysis was meant to primarily provide insight to the actual motion of the rotor.

III. Results

The experimental rig was run for several acceleration rates given non-dimensionally by α/ω_{cr}^2. Results for four runs are presented here: $\alpha/\omega_{cr}^2 = 7.88\times10^{-4}$, 1.64×10^{-3}, 6.38×10^{-3} and -8.18×10^{-4}. Acceleration rates were constant within 5% for runup while rundown rates were constant within 1%.

A typical waveform is shown in Fig. 2 ($\alpha/\omega_{cr}^2 = 7.88\times10^{-4}$). As can be seen, after the rotor passes through the critical speed the signal is a sinusoid at the operating speed, which has been modulated. The modulation is a result of the interaction of two frequencies (synchronous and critical speed) which produces a "beating". One purpose for the remainder of this paper is to further examine the transient response occuring at the two frequencies.

In Figs 3–6 the Bode diagrams are presented for the total non-dimensionalized motion (A/A_{cr}) for all four acceleration rates. Three phenomena occur as a result of acceleration:

(i) The maximum total amplitude is decreased with increasing acceleration.

(ii) The peak is shifted to higher operating speeds for higher accelerations and lower operating speeds for lower decelerations. For example, for $\alpha/\omega_{cr}^2 = 7.88\times10^{-4}$ the experimental maximum non-dimensionalized motion is 0.62 and occurs at $\omega/\omega_{cr} = 1.04$ while for $\alpha/\omega_{cr}^2 = 6.38\times10^{-3}$ the maximum amplitude is 0.28 and occurs at $\omega/\omega_{cr} = 1.16$. For comparison with no acceleration ($\alpha/\omega_{cr}^2 = 0.00$) the maximum response is 1.00 and occurs at $\omega/\omega_{cr} = 1.00$.

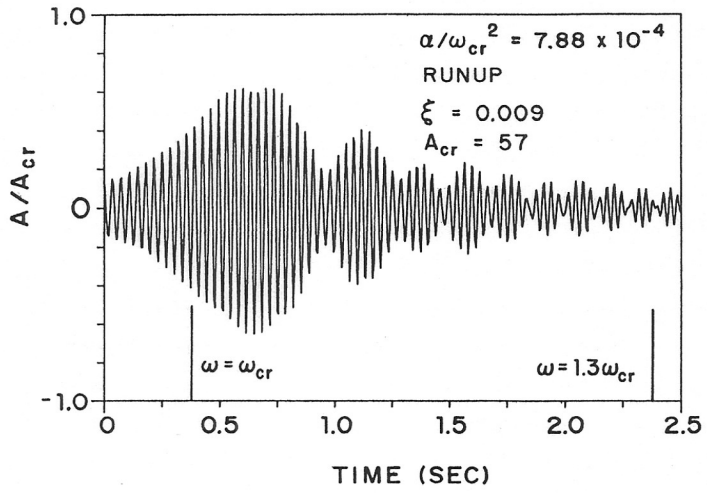

FIG. 2. Typical waveform as the rotor traversed the critical speed, $\alpha/\omega_{cr}^2 = 7.88\times10^{-4}$.

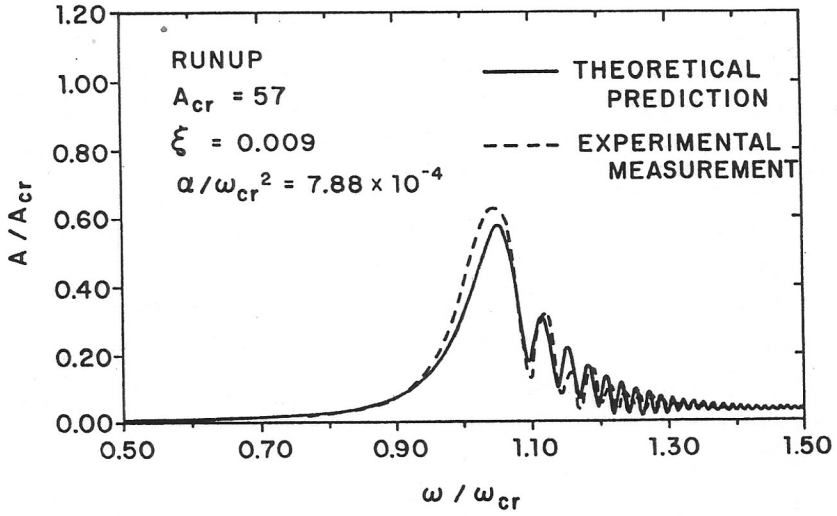

FIG. 3. Experimental total motion response and theoretical predictions, $\alpha/\omega_{cr}^2 = 7.88 \times 10^{-4}$.

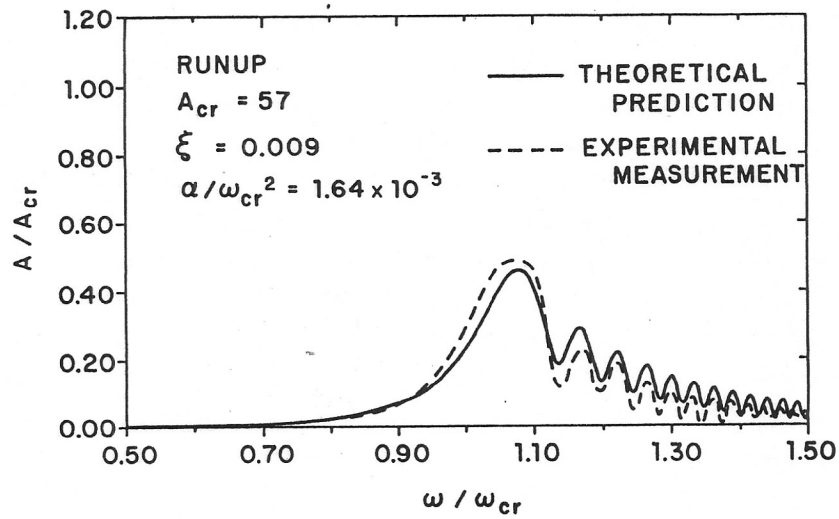

FIG. 4. Experimental total motion response and theoretical predictions, $\alpha/\omega_{cr}^2 = 1.64 \times 10^{-4}$.

(iii) A "beating" phenomenon appears in the total amplitude responses. This was also seen in the raw data (Fig. 2). Careful measurement shows that the "beating frequency" is approximately equal to $(\omega - \omega_{cr})$ $(\pm 5\%)$. This is easily explained by the presence of a component of motion occuring at the critical speed simultaneously with a component at the operating speed.

Also in Figs 3–6 comparison is made to the theoretical predictions from (5). As can be seen excellent agreement is obtained and differences in peak responses of 6% are found ($\alpha/\omega_{cr}^2 = 7.88 \times 10^{-4}$). Theoretical predictions also indicated the beating phenomena occured at the same frequency as observed experimentally.

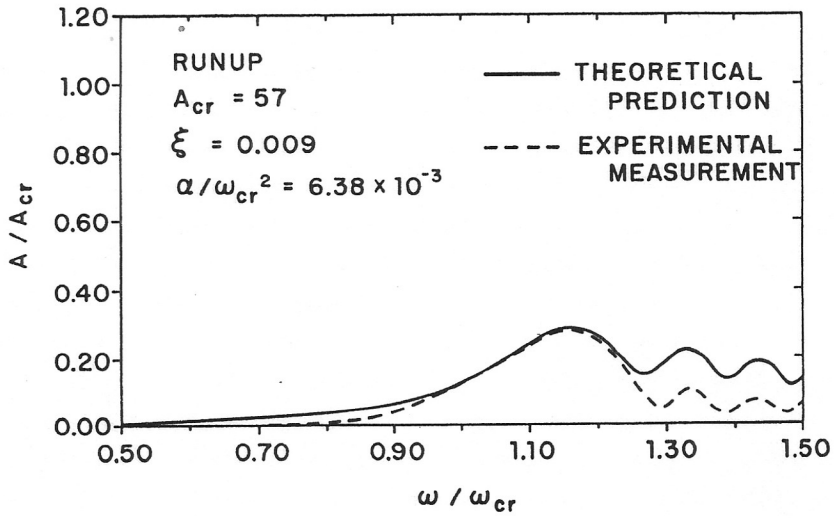

FIG. 5. Experimental total motion response and theoretical predictions, $\alpha/\omega_{cr}^2 = 6.38 \times 10^{-3}$.

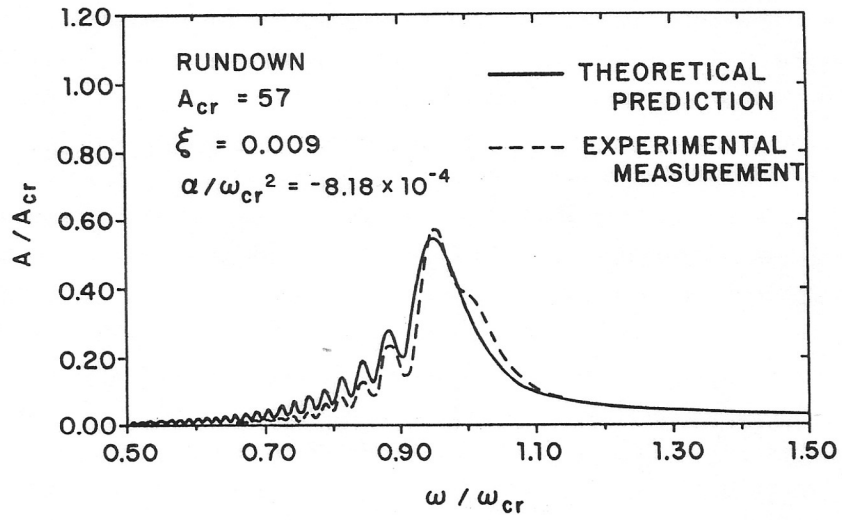

FIG. 6. Experimental total motion response and theoretical predictions, $\alpha/\omega_{cr}^2 = -8.18 \times 10^{-4}$.

In Fig. 7 a typical waterfall diagram is presented ($\alpha/\omega_{cr}^2 = 7.88 \times 10^{-4}$). This diagram shows the vibration spectra for a variety of operating speeds. The loci of two frequencies are noted: the critical frequency ($\omega/\omega_{cr} = 1.00$) and the synchronous frequency (ω/ω_{cr}). As the rotor is run up in speed, only one component is seen (synchronous) until the rotor reaches the critical speed. At the critical speed one large component is observed. On the post-critical speed spectra the two components are seen. The critical frequency component is seen to decay for large values of ω/ω_{cr}. The synchronous component remains constant in amplitude and represents the system unbalance eccentricity for large values of ω/ω_{cr}.

Vol. 310, No. 1, July 1980
Printed in Northern Ireland

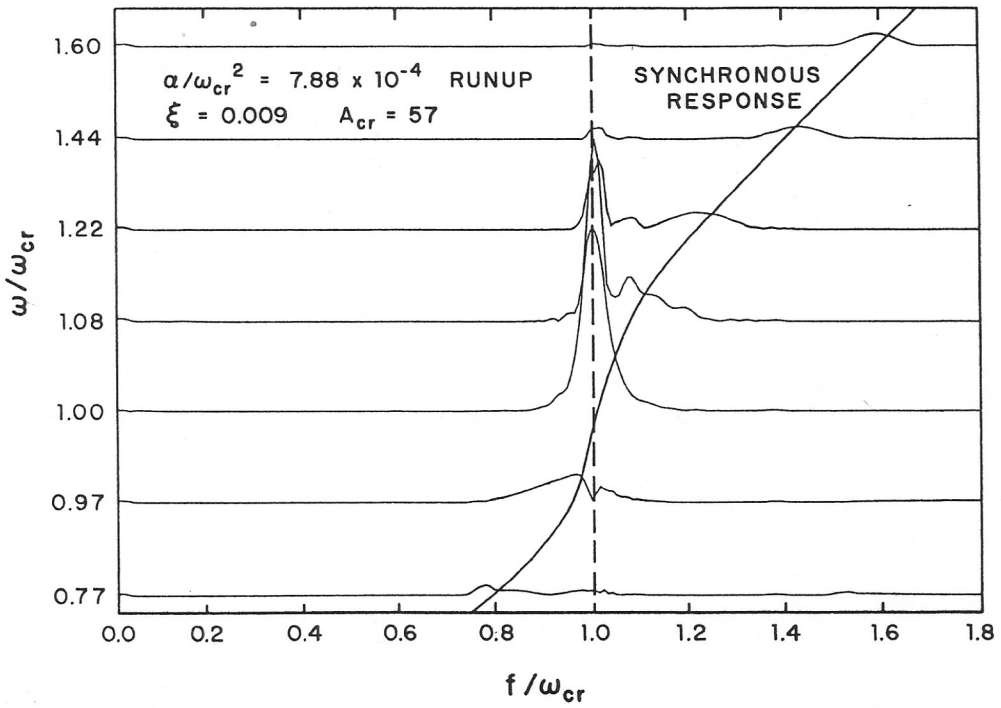

FIG. 7. Typical waterfall diagram, $\alpha/\omega_{cr}^2 = 7.88 \times 10^{-4}$.

In Figs 8–10 the non-dimensional amplitudes of the total, synchronous and critical speed components are shown as functions of ω/ω_{cr} for three typical runs. The total motion was previously presented and compared to theoretical predictions in Figs 3–6.

In any one of Figs 8–10 the synchronous response is seen to increase as the rotor speed approaches the critical speed and reach a maximum after the

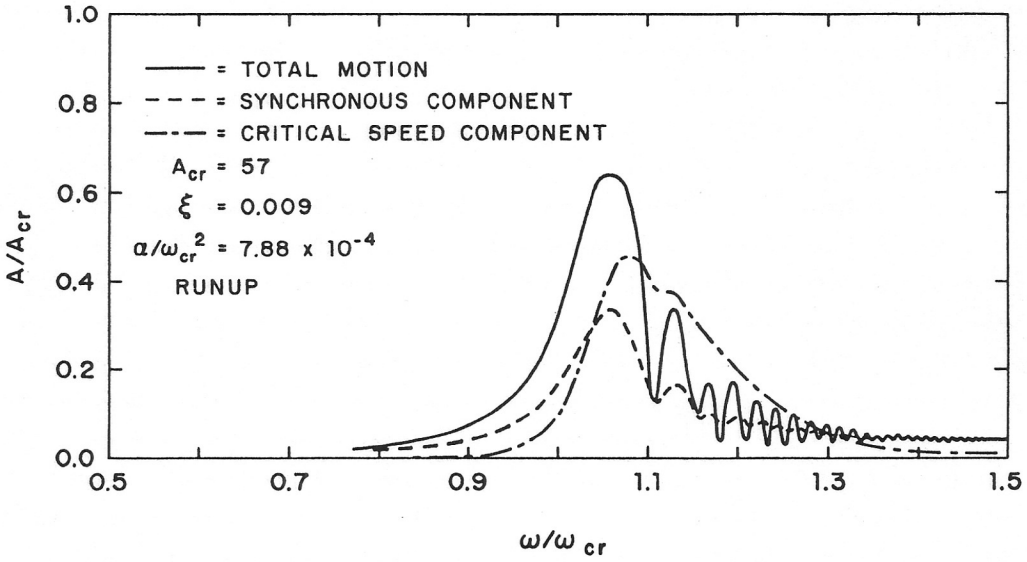

FIG. 8. Experimental total, synchronous and critical frequency response, $\alpha/\omega_{cr}^2 = 7.88 \times 10^{-4}$.

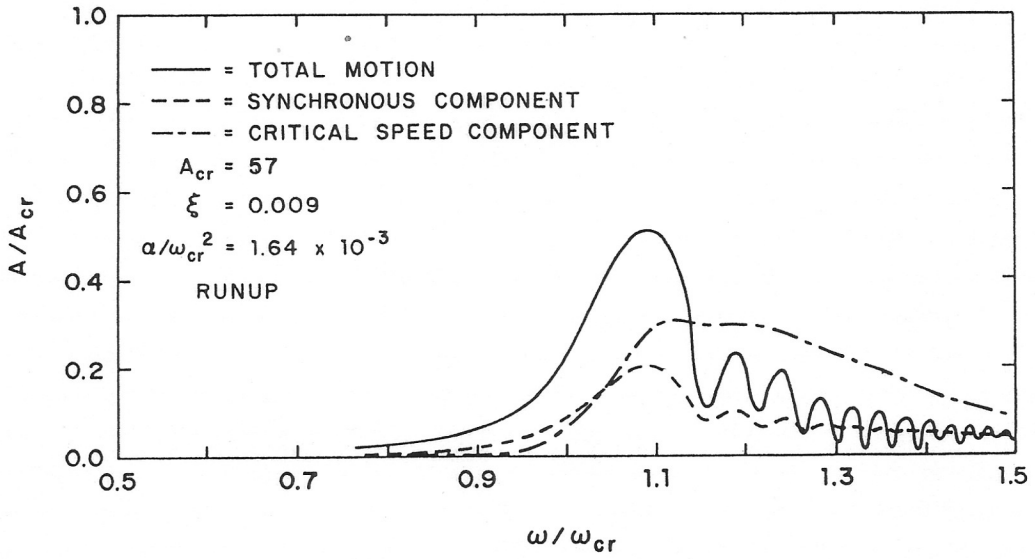

FIG. 9. Experimental total, synchronous and critical frequency response, $\alpha/\omega_{cr}^2 = 1.64 \times 10^{-3}$.

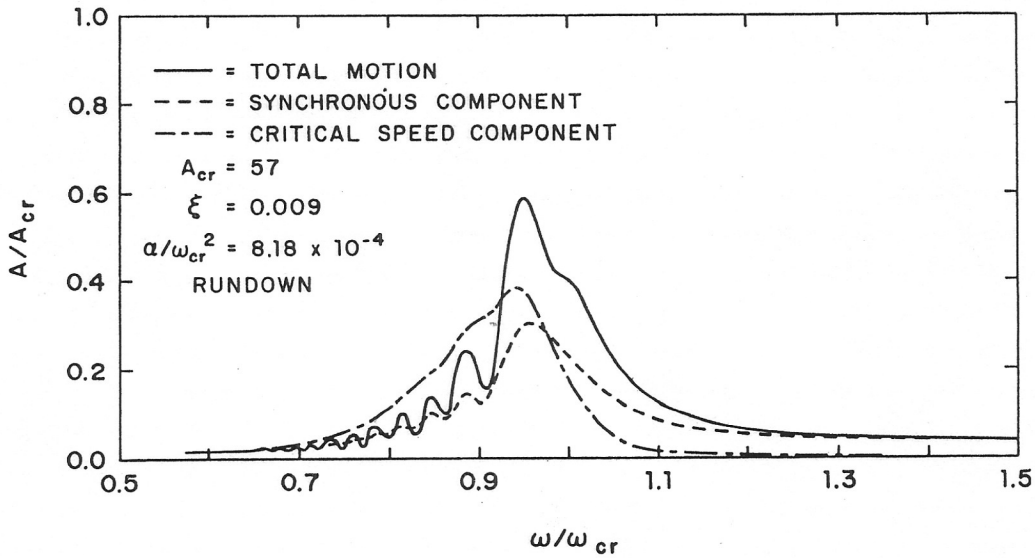

FIG. 10. Experimental total, synchronous and critical frequency response, $\alpha/\omega_{cr}^2 = -8.18 \times 10^{-4}$.

critical speed is passed. A small amount of "beating" is seen in these signals. Also, for large values of ω/ω_{cr} the synchronous response is seen to approach the unbalance eccentricity ($A/A_{cr} = 1/57$).

Also in any of these figures the critical speed component is seen to rise abruptly after the rotor traverses the critical speed and next decay exponentially. Thus, this free vibration is excited by the forced response for a small increment in time. If this explanation is to be accepted then the decay rate of this exponential should yield a damping ratio which corresponds to the value of

ξ measured previously for the system. For example, in Fig. 8 the logarithmic decrement was measured for the critical speed component between $\omega/\omega_{cr} =$ 1.15 and 1.30. From this measurement at the value of ξ was found to be 0.0091 which is within 4% of the average value of ξ found for the unaccelerated run (0.0088). Similar calculations for the other acceleration rates also were within 5% of $\xi = 0.0088$.

IV. Summary

In Figs 3–6 excellent agreement between the present experimental results and theoretical predictions (**5**) was found. Thus, the theory has been shown to be accurate in general. To summarize the effects of acceleration on a Jeffcott rotor, Figs 11 and 12 are presented. These were found using the theory in (**5**).

Figure 11 illustrates the maximum nondimensionalized excursion that a shaft undergoes as a function of acceleration ratio. Several values of system damping are included. Figure 11 represents the vibrational amplitude suppression (or in some cases the magnification) capabilities that accelerating a rotor through a critical speed presents. In Fig. 12 the nondimensionalized speed at which the maximum vibration occurs is presented as a function of α/ω_{cr}^2 for several damping ratios. Figure 12 thus represents the effect rotor acceleration has on the "observed critical speed".

For example, for a rotor with an acceleration ratio of 0.004 and a damping ratio of 0.01, one can expect a maximum response of 37% of an unaccelerated case and expect the maximum response at 1.08 times the critical speed. These effects are even more pronounced for lower values of ζ.

Also of interest from Figs 11 and 12 are the cases with large values of damping. For no acceleration ($\alpha/\omega_{cr}^2 = 0$) and a damping value of $\zeta = 0.25$, the

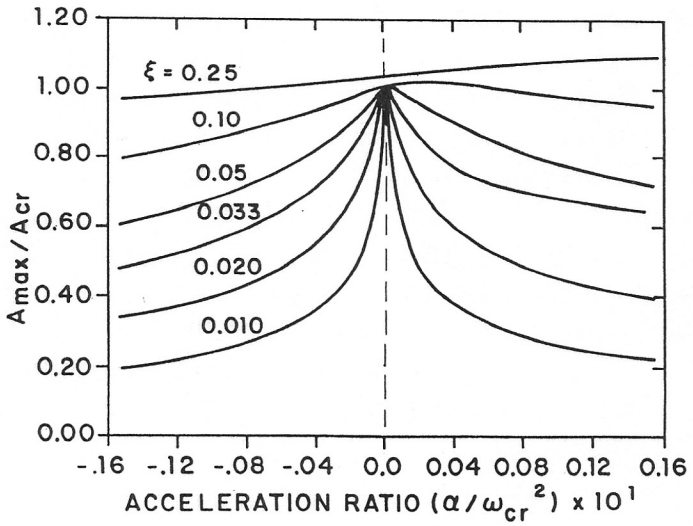

FIG. 11. Summary of maximum amplitude dependence on acceleration rate and damping.

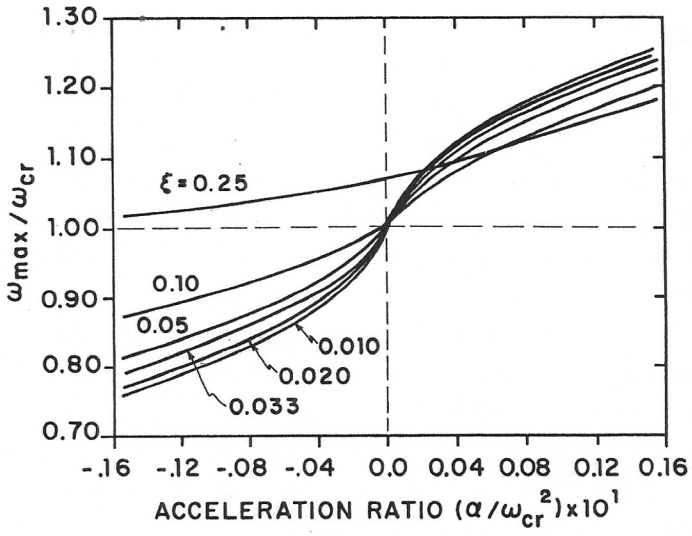

FIG. 12. Critical speed shift as a function of acceleration rate and damping.

value of A_{max}/A_{cr} is 1.04. The damped critical speed is at 1.07 times the undamped critical speed.

V. *Conclusions*

The effects of acceleration on a Jeffcott rotor have been experimentally determined. A small lightly damped rotor ($\zeta = 0.0088$) was instrumented and tested for a variety of acceleration rates. Synchronous tracking methods and fast Fourier transform frequency analyses were performed to interpret the data. Data compared to predictions from a previously developed method. Specific conclusions include:

(1) Differences between the theoretical and experimental results were less than 6%.

(2) A "beating" frequency was observed after the rotor traversed the critical speed. The "beating" is caused by the difference between the operating and critical speeds and is equal to $(\omega - \omega_{cr})$.

(3) Waterfall diagrams showed two distinct frequencies: synchronous and critical speed frequency.

(4) The critical speed frequency component was seen to decay exponentially. Measuring the logarithmic decrement yielded values of $\zeta = 0.0091$ which is within 4% of the actual damping of the unaccelerated rotor.

(5) Since the experimental data agreed with theoretical predictions for one value of ζ, responses were theoretically predicted for other damping ratios. Peak responses and the frequencies at which they occured were predicted for six typical values of ζ found on real machines and values of α/ω_{cr}^2 from -0.016 to 0.016 (also typical). Results indicate that the peak response can be reduced by four or more by using high acceleration rates with machines with low damping.

Acknowledgements

The authors wish to thank Dr. P. E. Allaire for his helpful discussions during this investigation. This research was sponsored by the Department of Energy under contract DE-AC01-79ET-13151, under the direction of Dr. D. W. Lewis, and the Industrial Supported Program for the Dynamic Analysis of Turbomachinery at the University of Virginia, under the direction of Dr. E. J. Gunter.

References

(**1**) R. M. Lewis, "Vibration During Acceleration Through a Critical Speed", *J. appl. Mech. Trans. ASME*, Vol. 54, pp. 253–257, 1932.

(**2**) J. G. Baker, "Mathematical-Machine Determination of the Vibration of an Accelerated Unbalanced Rotor", *J. appl. Mech. Trans. ASME*, Vol. 61, pp. A145–A150, 1939.

(**3**) R. B. Meuser and E. E. Weibel, "Vibration of a Non-linear System During Acceleration Through Resonance", *J. appl. Mech. Trans. ASME, Series E*, Vol. 15, pp. 21–24, 1948.

(**4**) R. Gasch, R. Markert and H. Pfützner, "Acceleration of Unbalanced Flexible Rotors Through the Critical Speeds", *J. Sound Vibration*, Vol. 63, pp. 393–409, 1978.

(**5**) H. L. Hassenpflug, R. D. Flack and E. J. Gunter, "Influence of Acceleration on the Critical Speed of a Jeffcott Rotor". Presented at the 1980 ASME Gas Turbine Conference. *J. of Engng. Power, Trans ASME*, Paper No. 80-GT-88.